ARTICLE

Beyond liquid crystals: new research trends for mesogenic molecules in liquids

Received 00th January 20xx,
Accepted 00th January 20xx

DOI: 10.1039/x0xx00000x

Martín Castillo-Vallés,[¥] Alejandro Martínez-Bueno,[¥] Raquel Giménez, Teresa Sierra and M. Blanca Ros*

Looking to understand the supramolecular assemblies that bring together certain molecules to form innovative functional materials with high-potential applications, the present review focuses on recent examples of molecular structures that are susceptible of stablishing self-assemblies both in bulk and in solvents.

This revision demonstrates that appropriate rod- and V-shaped, disc-like and star-shaped molecules as well as high-molecular-weight compounds, either dendrimers or polymers, exhibit a dual ability. Intermolecular interactions that provide liquid crystalline order in bulk may also manifest in solution and this allows to attain nanomaterials in the form of nanoaggregates. Through bottom-up approaches that involve the self-assembly of molecules driven by hydrogen bonding, π–π stacking, electrostatic or hydrophilic-hydrophobic interactions, appropriate molecules are able to induce a variety of thermotropic mesophases in bulk as well as aggregates with morphologies such as nanoparticles, nanofibers, nanorods or nanotubes in liquid media; including systems in which solvents are immobilized and form gel materials.

The aim of this work is to highlight the versatility of mesogenic molecules, that in turn opens the door to a wide number of possibilities, and therefore to help this topic to enter into a more mature period.

Introduction

There is growing interest in functional supramolecular materials, which are built through the self-assembly of molecules, and whose properties depend on their internal architecture.[1, 2] Control of the properties ultimately arises from molecular information and a major issue in this research area is therefore the design of the constituent units. These building blocks must fulfil self-assembly criteria, which concern intermolecular interactions, and also display functional properties, which ought to be transferred to the supramolecular assembly. With the aim of understanding the intermolecular interactions that bring together certain molecules to form such functional assemblies, we have considered two types of supramolecular materials.

Firstly, and given to our experience in this area, we have focused our attention on Liquid Crystals (LC) as a paradigmatic example of self-assembling systems.[3] LCs provide outstanding examples of supramolecular assemblies that allow access to functional materials formed by molecules that self-arrange and orient into architectures that define the final properties of the material.[4] The advantage of LCs lies in the vast design possibilities of their constituent units, i.e. mesogens. Mesogenic molecules contain information about self-organizational abilities but they can also encode optical, electronic or magnetic properties of technological interest that can be transferred to a variety of thermotropic liquid crystalline organizations, e.g., nematic, smectic, columnar and bent-core LCs amongst others.

Secondly, nanomaterials formed by the aggregation of molecular building blocks in liquid media have similar features such as a wide variety of chemical structures and tunable electronic and optical properties, which make them interesting for technological[5] or biomedical applications.[6] These materials are usually prepared by bottom-up approaches that involve the self-assembly of molecules driven by intermolecular interactions, such as hydrogen bonding, π–π stacking, electrostatic and hydrophilic-hydrophobic interactions, and they can exhibit different morphologies with low dimensionality such as nanoparticles, nanofibers, nanorods, nanotubes and others.

There is a lack of systematic studies in which these systems have been compared, but the two types of supramolecular material outlined above are closely related. In fact, the intermolecular interactions between mesogens can transcend the liquid crystal state and direct the formation of assemblies in a liquid medium. It is increasingly common in the literature to find reports of molecules that show liquid crystalline behaviour in bulk but are also able to form nanomaterials in solution with an internal molecular order similar to that of the mesophase. Such dual behaviour allows us to evaluate versatile molecules that can

Instituto de Ciencia de Materiales de Aragón (ICMA), Departamento de Química Orgánica-Facultad de Ciencias, Universidad de Zaragoza-CSIC, 50009 Zaragoza (Spain)

¥ These authors contributed equally to this work.

self-assemble in different environments, and it provides functional systems with defined molecular arrangements.

The present review focuses on recent examples of molecular structures that are capable of establishing intermolecular interactions both in bulk and in solvents, and therefore can give rise to thermotropic mesophases as well as nanoaggregates, respectively. The latter aggregates can also give rise to systems in which liquids are immobilized and form gels, a possibility that increases further their potential applications.

The aim of the review is to demonstrate that intermolecular interactions that provide liquid crystalline order in bulk can also manifest themselves in solution and this can lead to nanomaterials in the form of nanoaggregates, opening the door to new applications, as well as to help this topic to enter into a more mature period. For this purpose, representative examples that belong to the different molecular geometries and usually found in liquid crystals have been selected (Figure 1a). The literature reviewed span a decade, from the year 2009 to 2019, during which the following mesogenic structures have provided interesting examples that can illustrate the aforementioned dual behaviour. In this period of time, very few examples were found that concern the simplest rod-like or calamitic molecular structure. However, an increase in the number of terminal chains on a calamitic mesogens can provide, phasmids and polycatenary systems, which may yield a rich variety of mesophases that can be either calamitic, columnar or cubic. V-shaped molecules constitute the basic structure that forms the special type of bent-core liquid crystal organization with compact and polar packing or recently discovered mesophases, such as nematic twist-bend. Disc-like mesogens and star-shaped molecules mainly self-organize into columnar mesophases by π-stacking. Finally, high-molecular-weight mesogens, e.g. dendrimers or polymers, can give rise to liquid crystalline phases in which internal organization can be addressed by segregation of immiscible parts present in the molecules. A selection of packing models of the most representative liquid crystal phases of these mesogenic molecular designs are depicted in Figure 1b. The intermolecular interactions at play in these phases have been detected in solutions of these molecules in different solvents and thus nanoaggregates with defined internal structures have been described.

The review is organized in sections, each of which deals with one of the molecular structures cited above. The last section is devoted to the future outlook for these types of supramolecular systems and their potential as functional materials.

Calamitic molecules

Rod-shaped compounds, known as calamitic molecules in the liquid crystal field,[3] are composed of a rigid core and flexible alkyl side chains, and represent the first published and exploited family of molecules for a dual behaviour. However, few new reports are collected in the last ten years revised.

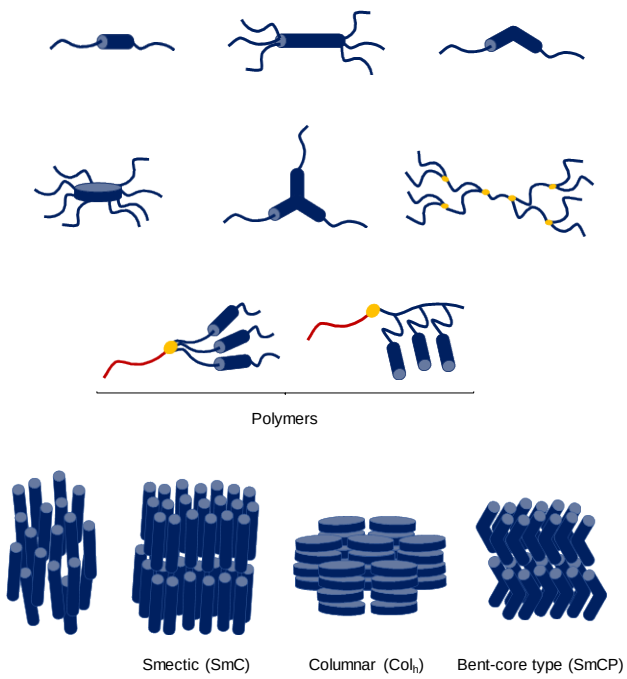

Figure 1. a) Representation of molecular geometries usually found in liquid crystals. b) Selection of packing models of representative liquid crystal phases considered in this review.

In this aim, cholesterol has been a commonly used building block in supramolecular chemistry thanks to its strong tendency to self-assemble via van der Waals forces. In fact, this biomolecule is very well-known in the field of liquid crystals since the oldest mesogen ever reported was a cholesterol derivative. With an appropriate molecular design, these molecules can also self-assemble in the presence of solvents. Actually, together with the van der Waals interactions, hydrogen-bonding has been proved to be an outstanding driving force for the formation of gels from cholesterol-containing molecules. Amide (**1**, Chart 1)[7, 8] and carbamate (**2**, Chart 1)[9] derivatives were reported to self-assemble into nanostructures when mixed with different liquids while the pure compounds showed the characteristic mesophases of the cholesterol unit, i.e. N*, SmA and SmC*. Other examples of cholesterol dimers, either connected by an alkyl flexible chain[10] or forming supramolecular complexes[11] also showed this dual performance.

Apart from cholesterol derivatives, another classical structural feature of calamitic mesogens, the incorporation of fluorinated chains, has been recently essayed.[12] in this respect, there are also few examples of molecules composed of a rigid aromatic core and fluorinated tails (**3a** and **3b**, Chart 1) that can form both nematic and smectic liquid crystalline phases and fibrillar assemblies that form gels in solvents. π-stacking of the cores and the intermolecular interactions between the fluorinated substituents are main intermolecular forces involved in both processes.[13, 14]

Recently, chiral rod-like mesogens in enantiomeric form as well as in mixtures (**4**, Chart 1) have been reported to self-assemble

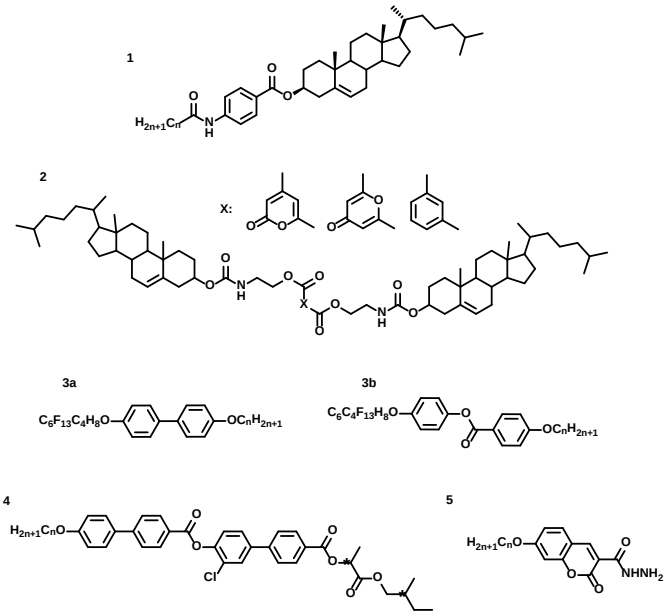

Chart 1. Chemical structures of selected calamitic molecules.

in appealing nanotubular morphologies when a concentrated solution was drop casted onto a substrate with a smectic crystalline order similar to that observed in the mesophase.[15] Finally, coumarin-based calamitic molecules (**5**, Chart 1) combined with the presence of a hydrazine group were described to self-assemble in the mesophase giving rise to smectic phases, while showing excellent gelation properties in many solvents of different polarities through strong hydrogen-bonding interactions.[16]

Phasmids and polycatenars

Non-conventional molecular shapes known as phasmidic or polycatenar[17] give rise not only to a broad variety of LC mesophases with high structural dependence, but to interesting self-assemblies in liquids. These compounds generally consist of a long aromatic rod-like core and multiple flexible chains at their ends. A selection of molecules with polycatenar and other similar shapes, such as swallow-tail, dumbbells, twin-tapered or related shapes, is covered in this chapter so as to reflect the varied molecular designs and functional groups found to endow these mesogens with added properties. With respect to LC behaviour, most of these compounds display columnar mesophases in which several molecules are arranged side-by-side in a columnar slice with segregation of the aromatic rigid core from the flexible terminal chains. The need for aggregation to form the columnar organization is in part a consequence of the molecular shape, as one molecule alone is usually unable to adopt the disc-shape required in conventional columnar mesophases. This aggregation occurs through a range of supramolecular interactions and can be directly related to the high tendency of a given compound to aggregate in solvents.

Typical polycatenar molecules with aliphatic chains and hydrazide groups[18,19] (**6**, Chart 2) make use of multiple hydrogen bonds to form columnar mesophases and stable organogels with a very low critical gelation concentration (0.06 wt%) and fluorescence that is enhanced upon aggregation (AIE effect). Interestingly, the structures of the organogels can be controlled by the polarity of the gelling solvent, as the molecules are arranged in a lamellar structure in the xerogel fibres formed in dichloroethane, but in rectangular columnar (Col_r) assemblies in fibres formed in ethanol.[20] Amide groups[21,22] also aid gelation in organic solvents by facilitating intermolecular H-bonding, with this process being particularly effective for 'hemiphasmidic' tapered mesogens derived from tropone,[23] imidazole[24] or pyrazole,[25, 26] which also arrange in multimolecular aggregates in the columnar mesophases. In particular, the compounds that bear a terminal pyrazole unit (**7**, Chart 2) give luminescent supergels in dodecane that show AIE

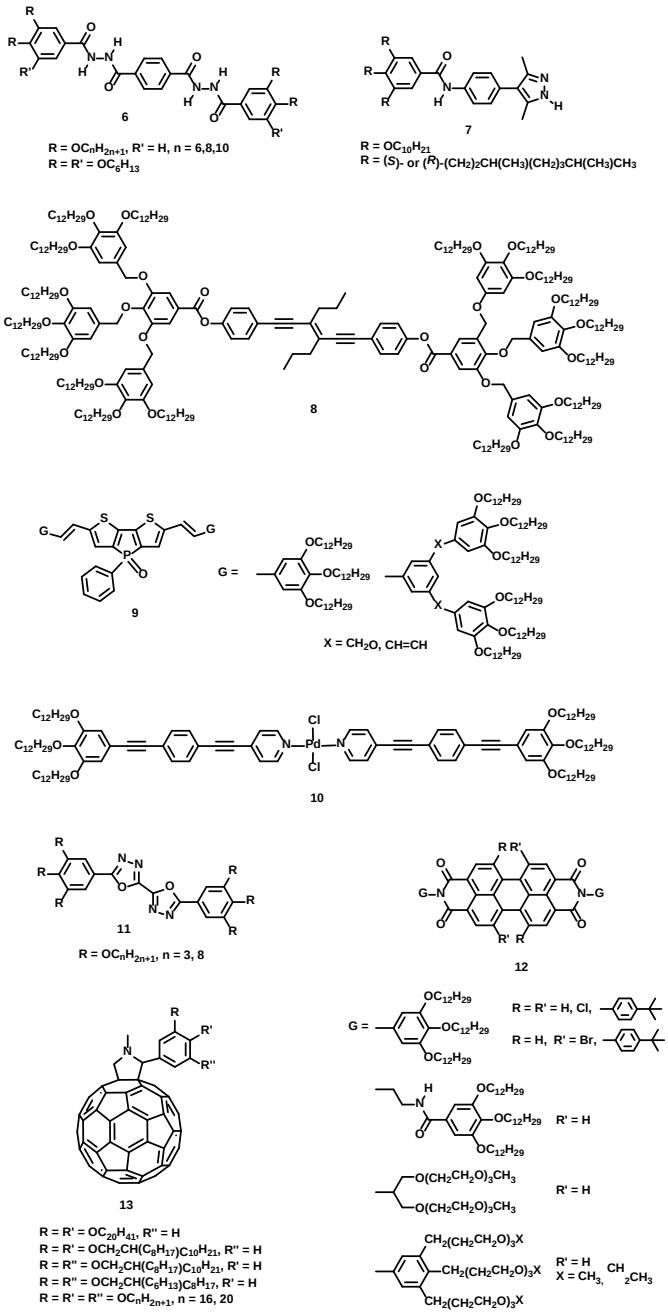

behaviour and they

Chart 2. Chemical structure of selected phasmids and polycatenars molecules

polymerise by a cooperative mechanism, with molecular chirality transferred to the gel fibres.[25]

Aggregation in solvents based exclusively on π- and van der Waals interactions was reported for dumbbell molecules bearing 3-hexen-1,5-diyne and dendritic wedges.[27-29] A molecule with a total of 18 chains (**8**, Chart 2) shows a unique columnar mesophase with a half-molecule per columnar stratum, and this aggregates in cyclohexane to give luminescent gels. Multifunctional phospholes with polycatenar or dumbbell shapes (**9**, Chart 2) also arrange to form highly luminescent Col_h mesophases and in polar organic solvents they can form gels whose photoluminescence can be tuned by variation of the solvent and the temperature.[30]

In another interesting example, in oligo(phenylenethynylene) (OPE) derivatives the important role of metallophilic Pd–Pd interactions was demonstrated (**10**, Chart 2). These interactions work cooperatively with π-stacking to form fibre aggregates with a high degree of internal order and single-molecule width.[31]

With the aim of obtaining nanostructured materials for optoelectronic applications, polycatenar structures containing electron-withdrawing units at the core were employed to obtain LC phases and luminescent organogels using only dipolar

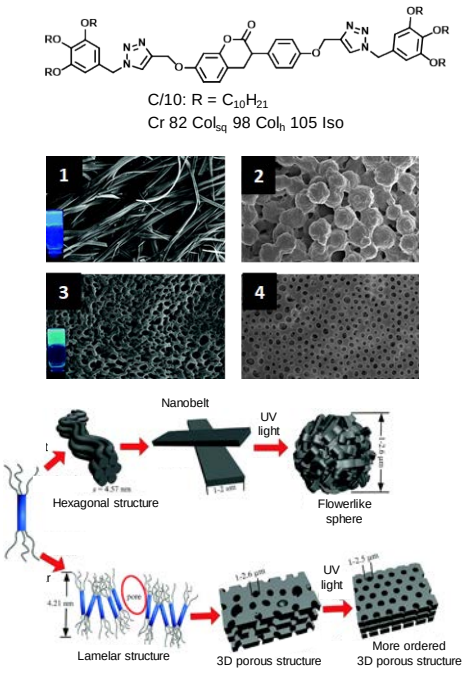

Figure 2. a) Chemical structure of the mesogen C/10. b) SEM images of the xerogels of mesogen C/10 obtained from acetone before irradiation (1) and after irradiation and standing in the dark (2), and xerogels obtained from n-hexane before irradiation (3) and after irradiation and standing in the dark (4). c) Schematic illustration of the possible formation mechanism of gels in acetone (top) or n-hexane (bottom). Adapted from Ref. 58 with permission from The Royal Society of Chemistry.

and π-interactions. This type of compound is exemplified by the twin-tapered bis-1,3,4-oxadiazoles,[32-35] oxadiazoles or thiadiazoles,[36] benzothiadiazole low bandgap compounds,[37-39] or fluorenones.[40] In particular, bis-1,3,4-oxadiazoles give rise to LC and gels with a helical structure and strong fluorescence (**11**, Chart 2).[32] Microbelt structures processed from an organogel have the optimum molecular arrangement to display fluorescent quantum yields close to unity and lasing properties with an ultralow amplified spontaneous emission (ASE) threshold.[34] In the fluorenone compounds the length of the terminal chain determines the LC behaviour, i.e., columnar or cubic micellar, and the morphology of their xerogels, i.e., fibrous or spherical.[40]

An important group of structures is those containing perylenebisimide (PBI). PBI dyes have excellent optical and n-type semiconducting properties combined with a high chemical stability. The strong tendency of these compounds to π-stacking facilitates the assembly of H- or J-type aggregates. Recent reviews on the subject have highlighted the broad variety of molecular structures with LC behaviour[41] and the relevant role of molecular and supramolecular engineering in PBI assemblies and functions.[42-44] Some representative examples are outlined below (**12**, Chart 2). Polycatenar mesogens substituted at the imide position aggregate in apolar solvents or gels through co-facial stacking.[45-50] Nanoggregates with different morphologies, either nanoparticles or nanobelts, were obtained on using solution-based methods with linear or branched substituted PBIs.[51] Remarkable efforts were focused on the study of the stability and dynamics of water-based PBI supramolecular systems[52] by using oligoethylene glycol-derived side chains as a water-solubilising group. It was found that the polarity of the substituents dictates the size, morphology, and optical properties of the aggregates.[47] Organisations similar to that observed in the helical columnar mesophases of dendronized PBIs[53, 54] were found for PBI amphiphiles in water, as elucidated by TEM, cryo-SEM and AFM.[55] With increasing concentration a fusion/fission process occurs in which nanorods composed of cofacially stacked molecules in a helical column merge to form nanoribbons in which the PBIs are arranged side-by-side. On using the same molecule and binary mixtures with a closely related compound, hydrogels with lower critical solution temperature (LCST) transitions and fibrillar morphology with internal columnar organization were obtained. At temperatures above the LCST water expulsion from the hydrogel occurs and this leads to a biphasic system with a columnar hexagonal mesophase, which triggers a colour change with fluorescence turn-on.[56] A different molecular design consisting of a PBI with free NH imide groups substituted with dendritic oligo(ethylene) groups at the bay position gives rise to a range of behaviours: Small aggregates (< 5 wt%), hydrogels (5-40 wt%), lyotropic liquid crystals (> 50 %wt) and a bulk thermotropic liquid crystal phase are all formed on increasing the concentration.[57] At low concentration the aggregates are amorphous and red-coloured, but on increasing the temperature they transform into blue-coloured triple-stranded helical aggregates with an unprecedented strongly coupled J-aggregation in which the transition dipole moment of PBIs is oriented parallel to the columnar axis.

Finally, additional functions were explored using photoresponsive moieties such as coumarin or azobenzene. A

group of coumarin hexacatenars with luminescent LC- and gel-forming properties show different aggregation schemes and morphologies in polar (acetone) or apolar (n-hexane) solvents. Furthermore, these compounds photodimerise upon irradiation with UVA light in both the LC and gel states.[58] The mesophase is retained but the gels transform into a solution, from which the gels reform with a different morphology upon standing in the dark (Figure 2). For some azobenzene polycatenars the photoisomerisation destroys the LC and gel properties in a reversible way[59, 60] or it changes the morphology of the aggregate, with long thin fibres transformed into shorter rods.[61] The power of poly-alkyl tails to promote dual self-assembly abilities has been also attractively described by Takanishi et al. for non-conventional molecular designs based on C60. Thus, the authors have reported various functional materials derived from alkylated fullerenes, namely alkyloxyphensubstituted N-methyl[60]fulleropyrrolidines (**13**, Chart 2), and they were able to obtain both SmC liquid crystalline phases and lamellar solvent-assisted aggregates with different morphologies.[62, 63, 64] Authors claimed that simple modifications in the substitution pattern of the alkyl tails, i.e. the degree of branching, length, number, and substitution position, as well as other experimental conditions, permitted to modulate the order and hardness/softness of the molecular assemblies, giving rise to many highly versatile series of disordered-to-ordered, rigid-to-soft materials.

V-shaped molecules

Numerous different chemical structures can fit the V-shaped description. One can consider the flexibility of the central core, the presence of polycatenar substituents at the end of the bent moiety, the length of the wings, the use of alkyl spacers within the arms of the V-shaped molecule, etc.

This variety of designs can be classified according to how the molecules are packed in the mesophase. Columnar arrangements are typically observed for V-shaped mesogens with polycatenar substituents either in the apex or at both ends of the V-structure. In these phases, several molecules interact to form a disc-like structure in which the aromatic V-structure is located in the core and the polycatenar coils are extended on the periphery. Consequently, π-π interactions and the segregation of the different parts of the molecule are responsible for the stacking of the discs to give rise to columns, in a similar way to the phasmids and polycatenars described in the previous section. Polycatenar bisphenylsulfone-based molecules represent one of the most widely explored families of columnar V-shaped mesogens. Yoshio, Kato and co-workers described the ability of these compounds to form columnar mesophases in bulk by π-π and dipole-dipole interactions (**14a** and **14b**, Chart 3).[65] A uniaxial orientation of the columns in the mesophase was achieved by applying an electric field. In addition, XRD studies confirmed that the organisation in the gel state was similar to that observed in the mesophase. Following Kato's work, several modifications have been introduced into the chemical structure of the bisphenylsulfone-based V-shaped mesogens by click chemistry (**14b**, Chart 3).[66-69] In most cases, these compounds present cubic and columnar phases in bulk and they act as good gelators in various solvents. The presence in the structure of triazole rings, which can act as N-donors, allowed the gels to be used as chemosensors and in water purification systems due to their ability to chelate transition metal ions and interact with other compounds. More simple and flexible dihydrazide derivatives also showed dual behaviour, with columnar arrangements both in the mesophase and in the gel state.[70, 71] With the aim of obtaining nanostructures in aqueous solutions, the introduction of hydrophilic poly(ethylene glycol) (PEG) chains has proven to be a good approach. Lee and co-workers reported a family of bent structures decorated with a PEG dendron grafted to their apex (**15**, Chart 3).[72-74] Six or more molecules formed macrocycles that stacked to form columnar mesophases. This arrangement was stabilised in water due to the presence of the hydrophilic dendrons and this system formed helical nanotubes in solution. In other attempts, PEG chains were directly linked to both ends of the V-structure.[75-77] It was reported that chiral aggregates were formed when chiral hydrophilic coils were used. Luminescent gels can be obtained by the introduction of oxadiazole and thiadiazole units into the V-shaped mesogens.

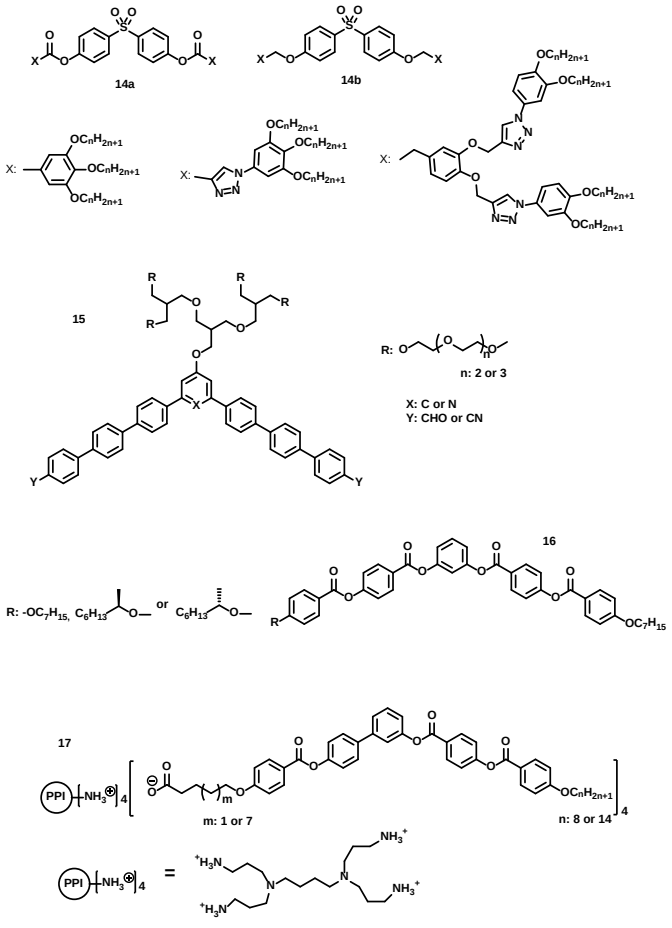

Chart 3. Chemical structures of selected V-shaped molecules.

Prasad, Das and co-workers reported a family of oxadiazole-containing mesogens that can establish strong π-π interactions,

which are responsible for the formation of columnar mesophases, aggregates in solution and very stable gels in non-polar solvents.[35] The introduction of stereogenic centres in the aliphatic chains led to helical ordering of the molecules both in the mesophase and in the aggregates in solution.[78] A high-performance organic light-emitting device was constructed with the latter compound, which exhibited bright green luminescence. In other work, polycatenar thiadiazole- and oxadiazole-based V-shaped mesogens were employed to obtain gels that showed an AIEE effect and were used as acid sensors.[79, 80]

Apart from these columnar arrangements, in the so-called bent-core liquid crystalline phases the bent molecules are forced to pack in a very compact manner, which precludes their rotation and leads to strong polar order along the bend direction. This packing is responsible for the very appealing properties of bent-core mesophases, i.e., polar organizations, induction of supramolecular chirality from achiral molecules, non-linear optical response and ferroelectric/antiferroelectric behaviour.[81, 82] Several attempts have been made to transfer the characteristic molecular order of bent-core mesophases (and therefore their properties) to other supramolecular systems. Ho, Hsu and co-workers described the ability of bent-core molecules to self-assemble in THF/water solutions to give rise to helical ribbons and nanotubes, despite the fact that achiral molecules were used (**16**, Chart 3).[83] It was demonstrated that the supramolecular chirality was induced by the bent structure of the molecule, since a linear analogue did not give a CD signal after aggregation. The stable packing of the bent molecules involves rotation of the carboxyl groups, and it induces a helical chain conformation that is responsible for the supramolecular chirality of the nanostructures in solution. As achiral molecules were used, both left- and right-handed helices were obtained. The introduction of chiral centres at the terminal alkyl chains (**16**, Chart 3) allowed the chirality to be controlled, as evidenced by mirror-imaged CD spectra when the R and S enantiomers were employed.[84] With similar objectives, Ros and co-workers synthesised a series of compounds that consisted of a hydrophilic poly(propylene imine) dendrimer joined to four hydrophobic bent-core structures (**17**, Chart 3).[85] The amphiphilic nature of such a dendritic structure could favour segregation in bulk and in solvents. Columnar and smectic liquid crystal phases were reported and aggregates were obtained in THF/water solutions. The length of the inner spacer and the terminal aliphatic chain seemed to play a crucial role in the formation of both the mesophases and nanostructures in solution.

The appropriate combination of short spacer and terminal alkyl chains allowed the formation of chiral superstructures, i.e., helical ribbons and nanotubes. SAXS of dried samples of the aggregates confirmed the smectic order of the molecules. Consequently, the authors proposed the formation of helical structures through local saddle-splay deformation of the lamellae, in a similar way to that observed in the B4 or helical nanofilaments (HNFs) phase.[86]

Moving on from aggregates in solution, several examples of gels formed by bent-core molecules have been reported in the literature. The compounds that form the aforementioned HNF phase in bulk warrant special attention. This phase has attracted

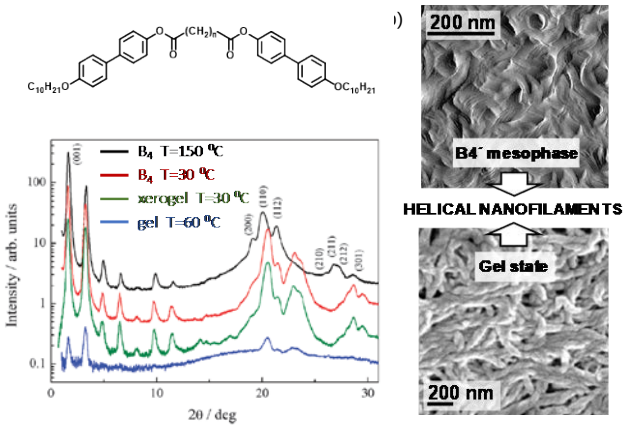

Figure 3. a) Chemical structure of the bent-core dimer. b) AFM image of the B4´ phase at room temperature (top) and SEM picture of xerogel in (–) menthone (bottom). c) X-ray pattern of the B4 and B4´phase, xerogel and gel in toluene. Adapted from Ref. 92 with permission from The Royal Society of Chemistry.

a great deal of attention because of its chiral nature and strong optical activity, despite the fact that it is formed by achiral molecules.[87] It has been reported that the helical nanofilaments that build this phase can host other mesogens while maintaining their morphology.[88] The ability of host solvents within the entangled filament network was first described by Clark and co-workers.[89] In addition to mixtures with small molecules and polymers, they also obtained stable gels of 1,3-phenylene bis[4-(4,9-alkoxyphenyliminonethyl)benzoate] (NOBOW) and hexadecane. The helical nanofilament morphology was preserved for mixtures with up to 98% hexadecane. This work proved that the B4 network can absorb a large amount of solvent. The layer spacing in the filaments was slightly increased in the gel state due to partial intercalation of hexadecane within the aliphatic chains of NOBOW. Gorecka and co-workers reported that the optical activity of the HNFs of these materials is not related to the helical conformation of the filaments but to the internal layer structure (layer optical activity).[90] The value of this parameter strongly depends on the number of stacked layers. The bent-core molecules exhibited both B4 phases and gels. SEM pictures of xerogels revealed the formation of helical ribbons made of mono- and bilayers, whereas up to 5–6 layers were stacked in the mesophase. Consequently, only bulk samples showed a clear Cotton effect in circular dichroism measurements.

Bent-core dimers are also suitable for gel formation. These molecular designs have been mainly explored with the aim of obtaining twist-bend nematic phases.[91] Gorecka's group described a series of dimers that formed HNF phases in bulk and also acted as excellent gelators in many solvents.[92] SEM pictures of xerogels revealed that the gels were formed by helical tubules of both handedness that resembled the morphologies of B4 mesophases in bulk observed by AFM (Figure 3b). Moreover, the X-ray pattern of the xerogel was similar to that of the mesophase, with seven periodic reflections related to a

robust lamellar order at the small angle region and several peaks at the wide angle region (Figure 3c). The authors therefore concluded that the fibres that formed the gel state had the structure of the bulk B4 phase. Moreover, the introduction of azo moieties into the wings of the dimers allowed light-responsive mesophases and gels to be obtained.[93] Monika et al. described another family of bent-core azo-dimers that were able to form gels in various organic solvents and cybotactic nematic phases in bulk.[94]

Star-shaped molecules

Star-shaped molecules are formed by a central core and three or more arms symmetrically attached by different types of linkers.[95] The nature of the core, the arms and the linker are important in the design since they control both the macroscopic and the microscopic properties. A vast number of star-shaped liquid crystalline molecules are formed by a rigid central core and three arms that can range from alkyl chains to conjugated rigid systems with aliphatic substituents at the periphery. Due to their form and their tuneable molecular design, star-shaped molecules can give rise to different types of mesophases, i.e., nematic, columnar or cubic, with columnar mesophases being the most common. These types of molecules are also capable of self-assembling in solution to give aggregates whose morphology and size can be controlled through molecule-molecule and molecule-solvent interactions.

Benzene-1,3,5-tricarboxamide (BTA) is one of the simplest star shaped cores and it has been extensively studied both in bulk and in solvents. The interest in BTAs is due to their well-defined helical 1D aggregates caused by the strong threefold α-helix-type intermolecular hydrogen bonding between amide groups.

Chart 4. Chemical structures of selected star-shaped molecules

In recent years, Meijer, Palmans and co-workers have introduced several modifications to the structure of BTAs to determine how they affect the intermolecular hydrogen bonding responsible for the bulk and solution properties. They altered the amide connectivity,[96] replaced the amide group by a thioamide,[97] changed peripheral alkyl chains by oligo(ethylene glycol)[98] or polydimethylsiloxane[99] in different ratios or separated the amide from the central benzene by introducing a methylene group.[100] Most of these compounds show liquid crystalline behaviour with hexagonal columnar mesophases and they form helical aggregates in organic solvents.

In the same way, Desmarchelier et al. generated a library of BTAs derived from dodecyl esters of amino acids.[101] The amino acid residue dictates the nature of the self-assembly in bulk, with hexagonal Col_h phases formed, and also in methylcyclohexane. The self-assembly process of BTAs can also be controlled by the introduction of stimulus-responsive units. Among the stimuli employed, light has attracted great interest because it can be applied in a localized way without modifying the chemical environment and it can produce reversible changes in the materials. Choi et al. designed a BTA molecule with peripheral light-responsive azobenzene units[102] (BTA-3AZO) with LC and gelation properties. This molecule shows a low-ordered Col_h LC phase, a highly ordered lamella-columnar, Col_L, LC phase and a lamello-columnar crystal phase. XRD patterns of the xerogel revealed the formation of lamellar superstructures with hexagonal columnar packing. Due to the presence of azo groups, organogels underwent sol-gel transitions when irradiated with UV light.

Electric fields have also been used to externally control the self-assembly process in columnar mesophases. Aida and co-workers designed a series of star-shaped molecules with a bowl-shaped chiral peptidic macrocycle as a central core attached to peripheral akyl chains with flexible amide spacers.[103] (**18**, Chart 4) These molecules were able to self-assemble into a nanoporous hexagonal columnar mesophase and homeotropic alignment was obtained when an electric field was applied. In addition, GPC and CD studies confirmed the ability of these macrocycles to self-assemble in cicolhexane[104].

Five-membered heterocyclic moieties can be employed as connectors instead of amide linkages and this change provides one-dimensional aggregates with electronic and luminescent properties in which π-π interactions are predominant. In this respect, oxadiazoles, thiadiazoles and triazoles have been the most widely explored groups. Das and co-workers designed and synthesised star-shaped molecules containing 3,4,5-oxadiazoles with alkoxy-substituted phenylenevinylene groups[105] and alkoxy-substituted phenyleneethynylenes[106] with different chain lengths (**19**, Chart 4). All of the compounds showed mesomorphic behaviour (columnar mesophases) and they formed gels in non-polar solvents. Depending on the concentration, phenylenevinylene compounds showed a hierarchical self-assembly in solution from spheres to fibres. Achalkumar and co-workers studied the different properties shown by 1,2,4-oxadiazole[107] and 3,4,5-thiadiazole[108] moieties

with respect to 1,3,4-oxadiazole. The number, length and position of the peripheral alkyl chains determined the

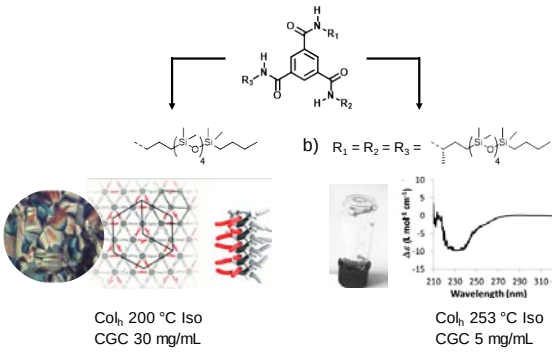

Figure 4. a) MOP texture and proposed superlattice of the hexagonal columnar mesophase. b) CD spectrum of the organogel in hexane. Adapted Ref. 99 with permission from Wiley-VCH.

mesomorphic properties of these compounds. Likewise, the gelification process showed a strong dependence on the number of alkyl chains at the periphery.

Triphenylamine, an electron-donor moiety with great potential in organic electronics,[109] has been used as a star-shaped unit to construct materials that show dual behaviour, namely as LCs in bulk and aggregates in solvents. Giusseppone and co-workers described star-shaped mesogenic molecules with a TPA core (**20,** Chart 4).[110] The presence of an amide linkage in one of the arms allowed the formation of columnar mesophases, the symmetry of which depended on the number and nature of the peripheral tails (Figure 4). These molecules undergo light-triggered supramolecular polymerisation in chlorinated solvents, a process common in other triphenylamine derivatives with an amide group.[111] The morphology of the resulting supramolecular polymers was studied by AFM and their form also depended on the number and nature of peripheral tails. Three-fold amide linkages between polycatenar benzoic acid and tris(aminophenyl)amine led to LC molecules that showed Col_h mesophases for molecules with six or more peripheral tails. The same molecules self-assembled in a variety of organic solvents to give gels with a wide range of minimum gelation concentrations, which depended on the solvent.[112]

Discotic molecules

Disc-shaped molecules are formed by a rigid aromatic core surrounded by flexible chains, which are commonly aliphatic in nature. The conjugated nature of the disc favours stacking of the molecules through π-π interactions to form columns in LC phases.[113] Among the wide variety of disc-like mesogens described in the literature, triphenylene is the most widely studied discotic core. The electron-donor character of triphenylene means that this planar polycyclic aromatic hydrocarbon has been extensively employed as a *p*-type semiconductor in columnar liquid crystals to obtain one-dimensional conductive materials with high hole mobilities.[114]

Interestingly, this mesogenic core also shows a high tendency to self-aggregate in solvents.[115] This dual behaviour was first described for a very simple asymmetrical hexasubstituted triphenylene with a terminal hydroxy group in one of the peripheral chains (**21**, Chart 5). The compound self-assembled to form Col_h mesophases in bulk and it formed two different kinds of fibrillar aggregates that gelled in ethanol depending on the temperature. As a consequence, other hexakisalkyl-substituted triphenylene derivatives have been explored. Despite its structural simplicity, some applications have been claimed for these materials both in solution and bulk. Commercial hexakishexyloxytriphenylene (HAT6) forms gels in an acetonitrile-based I^-/I^{3-} redox solution as the solvent to fabricate a solid electrolyte for dye-sensitised solar cells (DSSCs).[116] The HAT6 network prevented the evaporation of acetonitrile and also protected the device from the corrosive nature of the liquid electrolyte, thus increasing the lifetime of the photovoltaic system. The order provided by the triphenylene core has also been exploited for the orientation of gold[117] and CdS nanowires in ethanol aggregates.[118] Whereas doping with metallic nanostructures did not disrupt mesomorphism, the conductivity was increased by 3–4 times in the mesomorphic composite when compared to pure CdS.

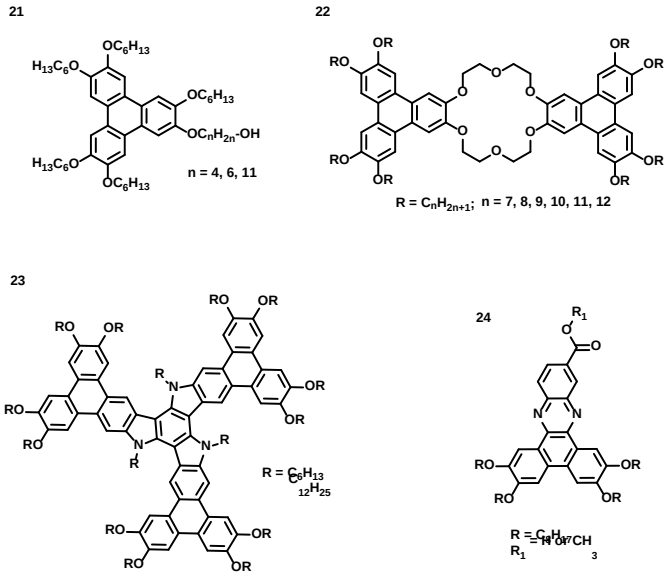

Chart 5. Chemical structures of selected discotic examples.

Modifications of the periphery surrounding the triphenylene may improve its aggregation capacity and open the door to new applications. Triazole-modified triphenylene LCs can form gels in cyclohexane, which has been successfully employed for sensing Cd^{2+} and nitroaromatic compounds.[119] On the other hand, triphenylene dimers linked by a crown ether (**22**, Chart 5) also proved to self-assemble in bulk and in solvents to form a gel state when doped with potassium counterions.[120] Large π-conjugated discotic cores of triphenylene-fused triazatruxenes (**23**, Chart 5) self-assembled to form columnar mesophases[121] and high hole mobilities were measured for these systems by the space-charge limited-current (SCLC) technique. Moreover,

the strong π-π

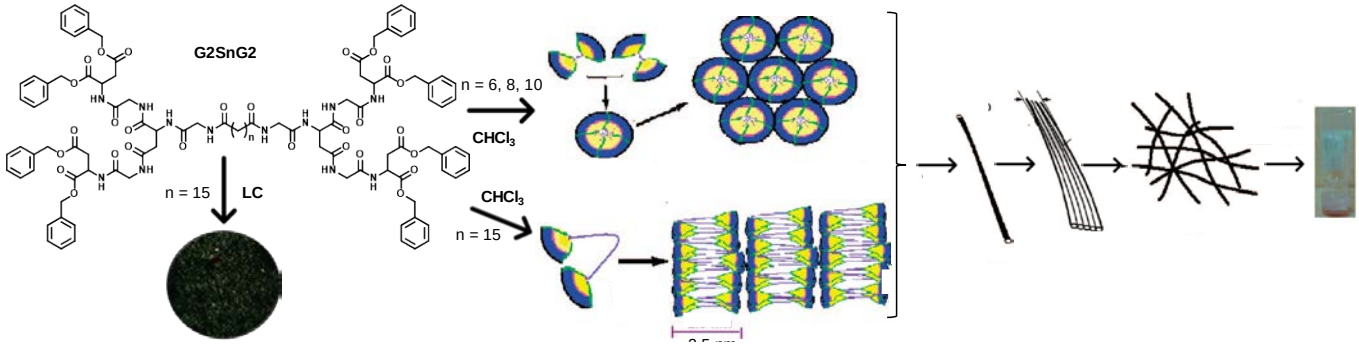

interactions between discs also served as a driving force for the formation of shrunken layer-like

Figure 5. Self-assemblies of aminoacid-based dendrimers: POM micrograph of the mesophase of G2S8G2 and schematic representations of the aggregates of the dendrimers in chloroform, from molecular packing to physical gels. Adapted with permission from Ref. 123 with permission from the American Chemical Society.

microstructures that led to gels in nonpolar hydrocarbon solvents and some aliphatic alcohols and esters.

Besides triphenylene, other discotic cores have been reported to combine mesomorphic behaviour and self-aggregation in solvents. For example, single dibenzo[a,c]phenazine derivatives (**24**, Chart 5)[122] and their dimers[123] show such dual behaviour as they form fluorescent columnar mesophases and gels. Discotic mesogens based on pyrene, a π-conjugated motif widely used in photonics and optoelectronics, allowed the formation of fluorescent mesophases and gels.[124] The photoluminescence wavelength of the pyrene core depended on the state of matter of the material, i.e., solid, liquid crystal or gel state. Remarkably, fibrillar gels from DMF were employed for the construction of OLED devices owing to their bulk electrical conductivity and emission properties.

Dendrimers

Dendrimers and dendrons are nearly monodisperse macromolecules characterised by a regular and highly branched structure with numerous available functional groups at their surface.[125] The controlled structure and multivalence of dendrons and dendrimers facilitates the tuning of their chemical structure, and this has been exploited to prepare materials that combine LC behaviour and self-aggregation in solvents.

Wedge-shaped dendrons based on amino acids have been reported to show such dual behaviour.[126, 127] As demonstrated by IR spectroscopy and pyrene inclusion experiments, H-bonds between amide linkages reinforced by π-interactions due to peripheral benzyl groups favour their gelating ability in numerous different solvents, with critical gel concentrations between 4 and 20 mg/mL. Thermotropic LC behaviour and gel-forming ability are observed for the second generation dendrons with an acrylate group at the focal point, which seems to reinforce π-interactions.[126] Changes in the amino acid composition have an influence on the mesophase arrangement.[127] Acrylic-G2gly–asp (Figure 5) shows a thermotropic Col_h phase and it is able to form gels in a variety of polar and non-polar solvents. The nanostructure of the xerogel maintains the Col_h arrangement of the thermotropic and this adopts a lamellar arrangement for Acrylic-G2ala–asp. However, in the presence of solvents, the aggregation into fibres that form gels is barely affected and the Col_h arrangement is observed. Dimeric molecules in which two glycine-aspartic acid dendrons are linked together through a flexible spacer retain the thermotropic LC properties of the dendrons and they can also form fibres in solvents, thus providing gels in chloroform at low concentrations, i.e., 3.5 mg/mL.[128] The length of the flexible spacer influences the inner molecular architecture of the fibres, which have a Col_h arrangement for shorter spacers (n = 6, 8, 10) and a lamellar arrangement for longer spacers (n = 15). For n = 10 and 15, the lamellar order is also present in bulk, whereas for n = 8, a cubic LC phase was identified. For n = 6, the mesophase arrangement could not be characterized.

Nanosegregation processes caused by the presence of moieties of different natures in the dendritic structure give rise to Janus dendrimers, which are useful to promote thermotropic LC

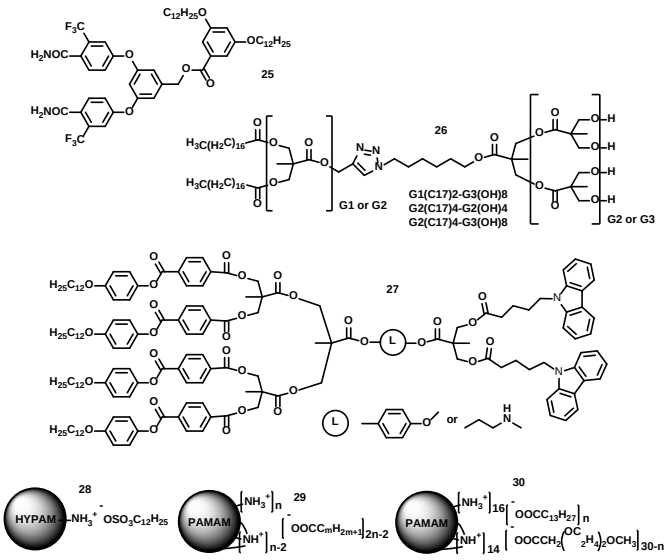

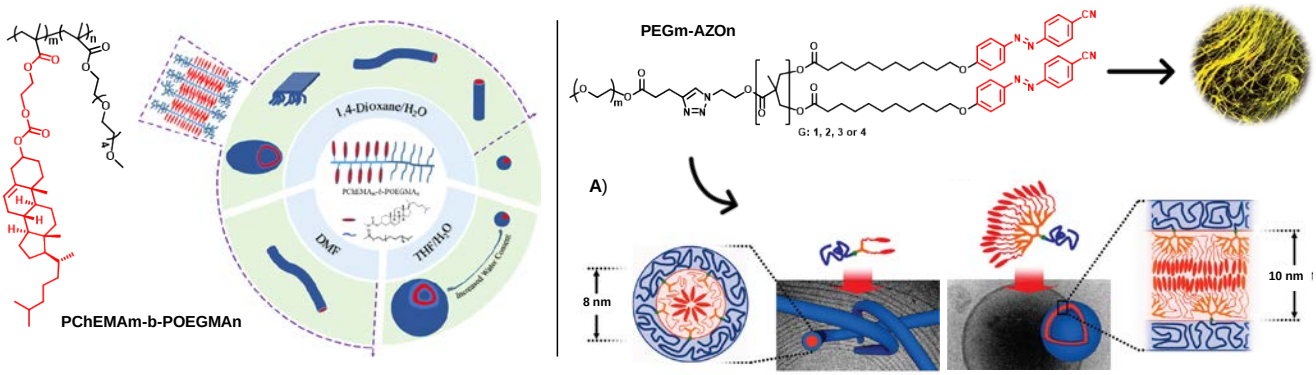

organisations and to self-assemble into nanostructures that are

Chart 6. Chemical structures of selected dendrimeric molecules.

Figure 6. Left: Schematic Illustrations of packing structures for self-assembled aggregates formed by the brush-like LC block copolymers PChEMAm-b–POEGMAn with different solvents. Adapted from Ref. 161 with permission of the American Chemical Society. Right: Self-assemblies of linear-dendritic diblock copolymers: POM micrograph of the mesophase of PEG114-AZO16 at 110 °C and schematic representations of the aggregates of PEG45-AZO2 (A) and PEG45-AZO16 (B) in water, together with the proposed models for the packing of the BCs in the polymeric self-assemblies. Adapted from Ref. 172 with permission from the American Chemical Society.

stable in solution or can gel a solvent. In particular, the combination of a polar dendron with an apolar dendron terminated with long hydrocarbon tails, provides a means to obtain lamellar mesophases along with the possibility of inducing self-aggregation into micelles, with the morphology depending on the nature of the solvent. In this respect, polybenzylether dendrons (**25**, Chart 6) with polar benzamide and trifluoromethyl groups combined with polycatenar dendrons have shown dual behaviour under certain conditions favoured by intermolecular H-bonding, van der Waals and π-interactions.[129] In particular, the dendrimer formed by first generation dendrons, G1-G1, which shows thermotropic LC behaviour, displays the most organized lamellar disposition within the xerogel fibres formed with a variety of solvents (e.g., hexane, toluene and 1-butanol, amongst others).

Amphiphilic Janus dendrimers built from 2,2-bis(hydroxylmethyloxy)propionic acid, bis-MPA (**26**, Chart 6), have also been shown to form thermotropic lamellar mesophases and micellar aggregates in water.[130] The elimination of intermolecular π-interactions still permits LC behaviour driven by segregation phenomena associated with the amphiphilic nature. The results of XRD studies showed a bilayer structure formed by interdigitation of long hydrocarbon tails, and this bilayer structure is also proposed to be present in the aggregates formed in water. Depending on the relative size difference between the hydrophilic and the lipophilic parts, the bilayer structure can bend and roll-up to form aggregates with different morphologies ranging from cylindrical micelles to vesicles or packed nanospheres.

A different approach to nanosegregation based on Janus dendrimers employed calamitic mesogenic units in one dendron and carbazole groups in the other Dendron (**27**, Chart 6).[131] In this case, π-interactions are mainly responsible for a lamellar organization that gives rise to SmC mesophases in the bulk. Apolar solvents such as cyclohexane promote aggregation into fibres at very low CGC, i.e., 0.25–1.00 wt%, and the layered nanostructure is maintained. Interestingly, this arrangement allows the electropolymerisation of the xerogel through carbazole groups and interesting optical effects related with aggregation-induced emission enhancement (AIEE) effects are observed.

Ionic interactions have also been employed to design amphiphilic dendrimers and this enables self-assembly in water. Depending on the structure of the counterions, these materials can also show thermotropic LC behaviour. PAMAM and PPI dendrimers contain a large number of protonatable inner and outer amino groups that can interact with negatively charged groups. PAMAM dendrimers can form ionic complexes with fatty acids (**29**, Chart 6) and these materials show SmA and columnar mesophases depending on the length of the acid and the number of protonated amine groups.[132,133] A lamellar arrangement in which the hydrophilic ionic region of the dendrimers wraps around a lipophilic region consisting of the long alkyl tails of the carboxylic acids seems to be the origin of the formation of nanoaggregates at concentrations of 5 mM. The resulting nanoobjects adopt different morphologies in aqueous media and can even encapsulate lipophilic molecules. The same type of behaviour in both the bulk and aqueous media was reported for HYPAM, a hyperbranched analogue of PAMAM, with dodecylsulfate as the counterion (**28**, Chart 6).[134] The possibility of using this type of nanoobject as a carrier for lipophilic drugs makes it interesting to explore their biocompatibility depending on their composition. Thus, ionic complexes of PAMAM and a combination of myristic acid (a lipophilic tail) and 2-[2-(2-methoxyethoxy)ethoxy]acetic acid (a hydrophilic tail) in different ratios were prepared (**30**, Chart 6).[135] This combination led to a SmA arrangement in the LC phase for the derivatives with a lipophilic/hydrophilic ratio above 10:20. Furthermore, the combination of both types of acid allowed modulation of the morphology of the nanoaggregates in water. Finally, it was observed that decreases in the content of myristic acid led to an increase in the biocompatibility of these nanoobjects, thus making them interesting as potential nanocarriers for lipophilic drugs.

Polymers

From high molecular weight compounds, polymers are probably the pioneers and the most widely studied compounds to date in terms of the versatile self-assembly potential of thermotropic liquid crystals in the presence of fluid media. Studies have mainly concerned block-copolymers (BCP) but a few homopolymers have also been reported that combine supramolecular abilities in bulk and in liquids (Chart 7). Among the homopolymers, different polymeric structures can show such dual behaviour. For example, the homopolypeptide poly-L-EG2-Glu forms a thermotropic LC phase and aggregates in water, although neither has been fully characterised. The morphology of the aggregates is either worm-like or fibre micelles depending on the molecular weight (**31**, Chart 7).[136] The amphiphilic mesogen-jacketed LC polymer POBP-7C promotes the formation of vesicles in water[137] and a mesogeniC (**32**, Chart 7) poly-biphenyl-methacrylate (PM6BiC18) is able to gel organic solvents (**33**, Chart 7)[138]

However, propelled by the synthetic advances in controlled polymerisations (ATRP, ROP, RAFT, etc), block-copolymers (BCP) have provided the most successful and versatile strategy in this area. For example, rod-coil copolymers that form flexible coil-like and rigid rod-like blocks, or amphiphilic block copolymers have been the first choice in investigating self-assembly behaviours. The differences between the segments – which mainly concern amphiphilic balance, π-π and dipolar interactions – drive anisotropic contacts between blocks to form liquid crystalline organization in bulk and solvent-mediated aggregation. Interestingly, it has been reported that the critical aggregation concentration (CAC) for BCPs is much lower than those for low molecular weight compounds. Additionally, aggregates from either liquid crystalline block-polymers or those including mesogenic blocks, both known as liquid crystalline block copolymers (LCBCPs), have been reported to be very stable, thus suggesting that the liquid crystal order arises from a kind of physical crosslinking that acts as a driving force for the generation of diverse morphologies and as a mechanism for moulding architectural materials from block polymers.[139]

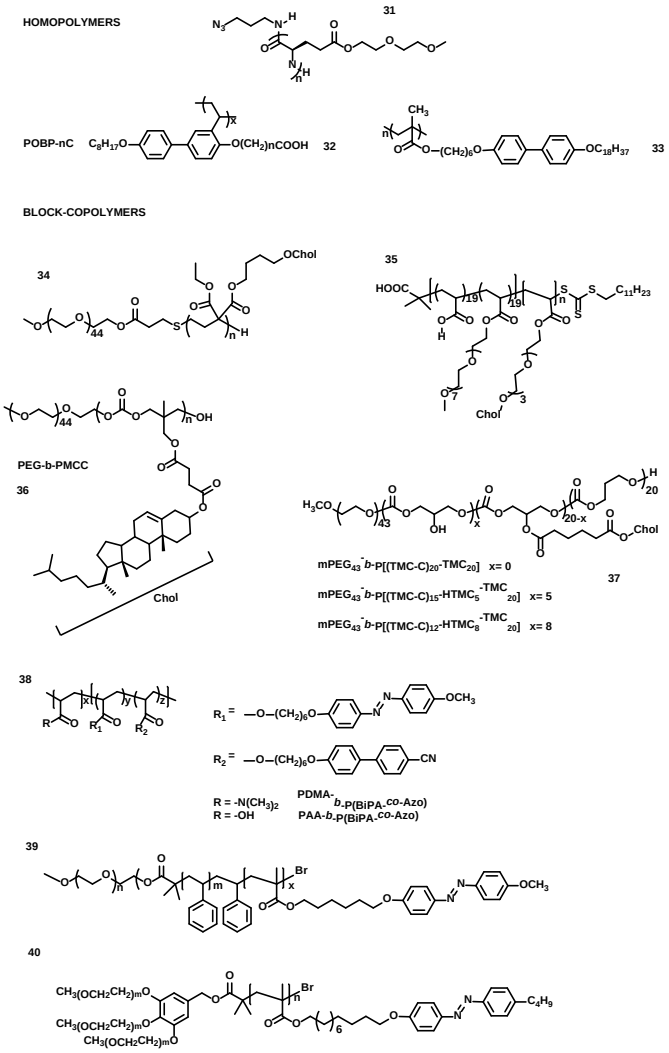

Chart 7. Chemical structures of selected polymers.

Several promesogenic structures have been considered for the design of LCBCPs. For example, the liquid crystalline poly(perfluorooctylethyl methacrylate) blocks proposed by Liu and co-workers[140] paved the way for the formation of core–shell cylindrical micelles.[141] Nevertheless, from the chemical design point of view, rod–coil block co-polymers are the most common systems and these are mainly built with flexible coil hydrophilic blocks based on polyethylene glycol (PEG or PEO), but also with poly(acrylic acid)[142-145] or poly(acrylamide)[142, 143, 146] segments. As far as the rod-blocks are concerned, well known mesogenic cores have been selected as a working guide and these range from cholesterol moieties, to ensure bio-applications, to azobenzene-based units when photo-responses were required. Furthermore, this methodology has inspired many approaches towards attractive nanoscale objects such as those described in focused reviews[147-150] or recent articles.[151]

Cholesterol is of interest in highly interdisciplinary research fields, as described in the first section of this work. The self-assembly of macromolecules bearing cholesteryl groups into LC phases (smectic, nematic, cholesteric or blue mesophases) has proven to be valuable in nanotechnology and related industries. However, at a biological level the role of cholesterol is also significant and well-studied and this offers broad possibilities and bio-applications for assemblies of amphiphilic cholesterol-based polymers, as discussed in recent reviews.[152-154]

A variety of amphiphilic block-copolymers with hydrophobic segments containing cholesterol-units have been reported in the last decade. These blocks are mainly responsible for promoting essentially nematic or smectic-like organizations in bulk as well as self-assemblies in solvents. For example, block copolymers based on PEG fragments, both as linear or brush-like structures derived from ethyleneoxide-acrylate or methacrylate monomers, have been explored by different authors. Li and co-workers carried out interesting research aimed at controlling the morphology of aggregates[155-160] (**34-36**, Chart 7) and they used cholesterol-based side-chain blocks. Depending on the weight fraction, the nature of both the hydrophobic and hydrophilic blocks and the solvents used[161] (Figure 6a), nanoribbons, nanofibres, nanotubes and spherical,

ellipsoidal and uncommon faceted vesicles were prepared for the first time from polymer vesicles[162] in aqueous solutions. Interestingly, rod-blocks formed the inner core of aggregates through the lamellar organization of cholesterol-units, generally in an interdigitated smectic A (SmA_d) structure in which, remarkably, the liquid-crystalline organization of the hydrophobic block in bulk is retained. Even though polybutadiene[155] or cyclopropane-1,1-dicarboxylates[157] (**34**, Chart 7) have been used as backbones, the majority of LCBCPs reported to date are based on acrylate or methacrylate backbones. However, as these backbones are not biodegradable, alternative backbone structures such as dextran[163] or polycarbonates[145, 164] (**37**, Chart 7) have recently been proposed and these have a notable effect on micellar morphologies and properties. In addition, tri-block copolymers have been employed to incorporate further hydrophilic portions to give brush-like copolymers, e.g., pH-sensitive polyacid-fragments, and this opens alternatives for controlled drug delivery systems.[142, 165]

When compared to changes in pH, solvent or temperature, light is a valuable stimulus because it can be applied locally and the response is rapid and does not require any modification in the chemical environment. In this respect, the azobenzene moiety has been incorporated in cases where photoresponsive materials were targeted. The azobenzene structure undergoes isomerisation between the *trans* and *cis* states upon appropriate irradiation and this causes polarity, size and shape changes that modify significantly the structures and properties of azobenzene-containing polymer blocks and hence the architectures of them.

Different azo-BCPs have been reported in the last decade and most of these contain flexible PEG-coils as hydrophilic blocks. Following most common AB_2 rod–coil designs, Li and co-workers reported polymersomes composed of LC rod-like azopolymers in layered membranes.[166-168] Interestingly, in addition to light, some of these membranes responded to various external stimuli – such as magnetic fields, electric fields and temperature – and this allowed controlled release induced by temperature variation.[168] Alternatively, the gelation abilities of various organic liquids have been reported for side-chain polyurethanes, which form amorphous fibrous aggregates that provide thermo- and photoreversible gels.[169] With respect to photoresponsive triblock-based polymers, it is worth highlighting spherical micelles from a poly(ethyleneoxide)-polystyrene-azocopolymer [PEO-b-PS-b–PMMAZO][170] or vesicles prepared with copolymers PDMA-b-P(BiPA-co-Azo) and PAA-b-P(BiPA-co-Azo)[143] (**38** and **39**, Chart 7).

The minimization of the interfacial energy, which is controlled by the balance of the hydrophilic/azo-hydrophobic block interaction, is the crucial driving force for the aggregation of these LCBCPs. Additionally, however, the preorganized branched architecture of the dendritic block has also been successfully evaluated for some new azo-based designs. It is worth highlighting different amphiphilic linear-dendritic block-copolymers,[171] particularly the mesogenic PEGm-AZOn series reported by Oriol and co-workers,[172, 173] which combine PEG chains of different molecular weights as hydrophilic segments and the first to fourth generations of azobenzene-containing dendrons based on bis-MPA as hydrophobic blocks (Figure 6b). The authors claimed that in comparison to other types of amphiphiles, for linear-dendritic BCs with a hydrophobic rigid dendritic block the aliphatic dendritic matrix was flexible enough to enable the reorganization of the mesogenic azobenzene moieties during aggregation. This is a key point for obtaining self-assemblies with different morphologies. Thus, depending on the generation of the dendritic moieties, aggregation in aqueous solutions gave rise to cylindrical micelles (nanofibres), sheet-like aggregates, tubular micelles, or photoresponsive polymersomes.[172] Alternatively, star-block copolymers $3PEO_m$-b-$PMAAz_n$ that combine a three-armed poly(ethylene oxide) segment and a side chain azobenzene-poly(methacrylate) block (**40**, Chart 7) have recently been reported. These materials form stable spherical micelles with clear lamellar stripes and the size is influenced by the self-assembly conditions and the lengths of two blocks.[174] Interestingly, according to the authors´ comments, the mesogenic character (SmA) of the block-copolymers occurs on aggregation regardless of the number of arms, from one to three, in the hydrophilic block.

Conclusions and outlook

The recent investigations highlighted in this review have demonstrated that there is growing interest in the study of mesogenic molecules in liquids and their potential applications of these systems.

A wide variety of thermotropic LCs with almost any kind of molecular shape (rod-like, polycatenar, V-shaped, disc-like, star-shaped; as well as high-molecular-weight LCs, i.e., dendrimers or polymers) have been reported to aggregate in liquids. This process occurs through the self-assembly of molecules driven by hydrogen bonding, π-π stacking, electrostatic interactions or hydrophilic-hydrophobic interactions. Appropriate molecules are able to provide liquid crystalline order in bulk, and may also self-assemble in liquids to form nanoaggregates with varied morphologies such as nanoparticles, micelles, vesicles, nanofibers, nanorods, nanotubes, etc. In addition, a great variety of examples rely on the ability to form gel materials.

Regardless of the molecular shape and resulting properties, interesting trends in research are worth highlighting, such as the study of the aggregation of mesogens with fluorescent units. This type of molecule give rise to photoluminescent gels or nanoaggregates whose emission can be tuned by aggregation, temperature or other stimuli. Poly(ethylene glycol)-substituents are a common motif for mesogens with interesting aggregation phenomena in water-based solvents. It is also worth noting that photoresponsive azobenzene-containing LCs were shown to form switchable morphologies upon irradiation. Finally, chiral aggregates with well-organised helical columns or a lamellar structure in the form of nanofibers

or nanotubes can be obtained, the last ones from achiral bent-core molecules.

Despite the number of reports, some of which relato to with significant achievements – such as those outlined above –, many examples are merely descriptive of the dual behaviour and this highlights the lack of systematic studies to correlate the self-organization in bulk or solvents. Nevertheless, this gap can be addressed in the future by developing standardized procedures and using available experimental techniques that would allow detailed characterization. This approach would offer the possibility of studying the relationships between the molecular structure, the self-assembly and their optical, electrical, magnetic and mechanical properties.

In spite of the many unknown aspects, this is a field with great potential in nanoscience research. The final goal should be to translate in a controlled way the molecular order of LC phases to the nanoaggregates in solvents as an alternative to process in the thermotropic LC phases. Moreover, the molecules can be modified with functional units to obtain complex and highly functional systems with structure at the nanoscopic scale. A wide variety of solvents can be used for such processing, including the as-yet unexplored ionic liquids or LC phases as the fluid media.

It is clear that the acquired knowledge from the LC field and the potential to develop a new generation of functional materials[175] could be further exploited in other varieties of supramolecular materials using the same molecules in liquids This could open up new processing alternatives and applications for supramolecular functional materials.

Conflicts of interest

There are no conflicts to declare.

Acknowledgements

The authors thank MICINN-FEDER funds (projects: MAT2015-66208-C3-1-P and PGC2018-093761-B-C31; M. C.-V. fellowship: BES-2016-078753) and the Gobierno de Aragón-FSE (E47_17R) for financial support.

Notes and references

1. *Supramolecular Chemistry: from molecules to nanomaterials*, Ed. J. W. Steed and P. A. Gale, Wiley-VCH, Weinheim, 2012.
2. D. B. Amabilino, D. K. Smith and J. W. Steed, *Chem. Soc. Rev.*, 2017, **46**, 2404-2420.
3. *Handbook of Liquid Crystals*, J. W. Goodby, P. J. Collings, T. Kato, C. Tschierske, H. F. Gleeson and P. Raynes, Wiley-VCH, Weinheim, 2014.
4. T. Kato, J. Uchida, T. Ichikawa and T. Sakamoto, *Angew Chem Int Ed Engl*, 2018, **57**, 4355-4371.
5. S. Kundu and A. Patra, *Chem. Rev.*, 2017, **117**, 712-757.
6. P. Xing and Y. Zhao, *Adv. Mater.*, 2016, **28**, 7304-7339.
7. K. Kubo, K. Tsuji, A. Mori and S. Ujiie, *J. Oleo Sci.*, 2014, **63**, 401-406.
8. K. Kubo, K. Tsuji, S. Ujiie and A. Mori, *Chem. Lett.*, 2014, **43**, 568-570.
9. T. Michinobu, K. Hiraki, N. Fujii, K. Shikinaka, Y. Katayama, E. Masai, M. Nakamura, Y. Otsuka, S. Ohara and K. Shigehara, *Bull. Chem. Soc. Jpn.*, 2011, **84**, 667-674.
10. G. Shanker and C. V. Yelamaggad, *J Phys Chem B*, 2011, **115**, 10849-10859.
11. Q. Hou, S. Wang, L. Zang, X. Wang and S. Jiang, *J. Colloid Interf. Sci.*, 2009, **338**, 463-467.
12. M. Hird, *Chem. Soc. Rev.*, 2007, **36**, 2070-2095.
13. B. Cao, S. Hayashida, Y. Morita and H. Okamoto, *Mol. Cryst. Liquid Cryst.*, 2016, **632**, 49-56.
14. B. Cao, Y. Kaneshige, Y. Matsue, Y. Morita and H. Okamoto, *New J. Chem.*, 2016, **40**, 4884-4887.
15. V. Novotná, V. Hamplová, L. Lejček, D. Pociecha, M. Cigl, L. Fekete, M. Glogarová, L. Bednárová, P. W. Majewski and E. Gorecka, *Nanoscale Adv.*, 2019, **1**, 2835-2839.
16. P. Chen, Y. Li, X. Chen and Z. An, *Liq. Cryst*, 2012, **39**, 1393-1401.
17. J. Malthête, H. T. Nguyen and C. Destrade, *Liq. Cryst.*, 1993, **13**, 171-187.
18. P. Zhang, H. Wang, H. Liu and M. Li, *Langmuir*, 2010, **26**, 10183-10190.
19. S. N. Qu, H. T. Wang, Z. X. Yu, B. L. Bai and M. Li, *New J. Chem.*, 2008, **32**, 2023-2026.
20. B. L. Bai, C. X. Zhang, J. Wei, J. Ma, X. L. Lin, H. T. Wang and M. Li, *RSC Adv.*, 2013, **3**, 12109-12116.
21. E. Díaz, E. Elgueta, S. A. Sánchez, J. Barberá, J. Vergara, M. Parra and M. Dahrouch, *Soft Matter*, 2017, **13**, 1804-1815.
22. Y. T. Shen, C. H. Li, K. C. Chang, S. Y. Chin, H. A. Lin, Y. M. Liu, C. Y. Hung, H. F. Hsu and S. S. Sun, *Langmuir*, 2009, **25**, 8714-8722.
23. M. Hashimoto, S. Ujiie and A. Mori, *Adv. Mater.*, 2003, **15**, 797-800.
24. S. H. Seo, J. H. Park and J. Y. Chang, *Langmuir*, 2009, **25**, 8439-8441.
25. S. Moyano, J. L. Serrano, A. Elduque and R. Gimenez, *Soft Matter*, 2012, **8**, 6799-6806.
26. S. Moyano, J. Barberá, B. E. Diosdado, J. L. Serrano, A. Elduque and R. Giménez, *J. Mater. Chem. C*, 2013, **1**, 3119-3128.
27. A. Pérez, J. L. Serrano, T. Sierra, A. Ballesteros, D. de Saa and J. Barluenga, *J Am Chem Soc*, 2011, **133**, 8110-8113.
28. A. Pérez, J. L. Serrano, T. Sierra, A. Ballesteros, D. d. Saá, R. Termine, U. K. Pandey and A. Golemme, *New J. Chem.*, 2012, **36**, 830-842.
29. A. Pérez, D. de Saa, A. Ballesteros, J. L. Serrano, T. Sierra and P. Romero, *Chem. Eur. J.*, 2013, **19**, 10271-10279.
30. C. Romero-Nieto, M. Marcos, S. Merino, J. Barberá, T. Baumgartner and J. Rodríguez-López, *Adv. Funct. Mater.*, 2011, **21**, 4088-4099.
31. M. J. Mayoral, C. Rest, V. Stepanenko, J. Schellheimer, R. Q. Albuquerque and G. Fernandez, *J. Am. Chem. Soc.*, 2013, **135**, 2148-2151.
32. S. Qu, L. Zhao, Z. Yu, Z. Xiu, C. Zhao, P. Zhang, B. Long and M. Li, *Langmuir*, 2009, **25**, 1713-1717.
33. S. Qu, L. Wang, X. Liu and M. Li, *Chem. Eur. J.*, 2011, **17**, 3512-3518.
34. S. Qu, H. Wang, W. Zhu, J. Luo, Y. Fan, L. Song, H.-X. Zhang and X. Liu, *J. Mater. Chem.*, 2012, **22**, 3875-3881.
35. A. P. Sivadas, N. S. Kumar, D. D. Prabhu, S. Varghese, S. K. Prasad, D. S. Rao and S. Das, *J. Am. Chem. Soc.*, 2014, **136**, 5416-5423.

36. B. Pradhan, V. M. Vaisakh, G. G. Nair, D. S. S. Rao, S. K. Prasad and A. A. Sudhakar, *Chem.-Eur. J.*, 2016, **22**, 17843-17856.
37. D. Huang, M. Prehm, H. Gao, X. Cheng, Y. Liu and C. Tschierske, *RSC Adv.*, 2016, **6**, 21387-21395.
38. H. Fang, H. Gao, T. Wang, B. Zhang, W. Xing and X. Cheng, *Dyes and Pigments*, 2017, **147**, 190-198.
39. B. Zhang, Y. Xiao, H. Fang, H. Gao, F. Wang and X. Cheng, *New J. Chem.*, 2018, **42**, 16709-16716.
40. K. Zhao, Y. Xiao, C. Guo, Q. Chang, H. Gao and X. Cheng, *Tetrahedron*, 2019, **75**, 409-415.
41. R. K. Gupta and A. A. Sudhakar, *Langmuir*, 2019, **35**, 2455-2479.
42. F. Wurthner, C. R. Saha-Moller, B. Fimmel, S. Ogi, P. Leowanawat and D. Schmidt, *Chem Rev*, 2016, **116**, 962-1052.
43. Z. Guo, X. Zhang, Y. Wang and Z. Li, *Langmuir*, 2019, **35**, 342-358.
44. F. Wurthner, T. E. Kaiser and C. R. Saha-Moller, *Angew Chem Int Ed Engl*, 2011, **50**, 3376-3410.
45. Z. Chen, V. Stepanenko, V. Dehm, P. Prins, L. D. Siebbeles, J. Seibt, P. Marquetand, V. Engel and F. Wurthner, *Chem. Eur. J.*, 2007, **13**, 436-449.
46. Z. Chen, U. Baumeister, C. Tschierske and F. Wurthner, *Chem. Eur. J.*, 2007, **13**, 450-465.
47. J. Schill, L. G. Milroy, J. A. M. Lugger, A. Schenning and L. Brunsveld, *ChemistryOpen*, 2017, **6**, 266-272.
48. X. Q. Li, V. Stepanenko, Z. Chen, P. Prins, L. D. Siebbeles and F. Wurthner, *Chem. Commun.*, 2006, 3871-3873.
49. S. Ghosh, X. Q. Li, V. Stepanenko and F. Wurthner, *Chem. Eur. J.*, 2008, **14**, 11343-11357.
50. F. Würthner, C. Bauer, V. Stepanenko and S. Yagai, *Adv. Mater.*, 2008, **20**, 1695-1698.
51. K. Balakrishnan, A. Datar, T. Naddo, J. Huang, R. Oitker, M. Yen, J. Zhao and L. Zang, *J. Am. Chem. Soc.*, 2006, **128**, 7390-7398.
52. D. Gorl, X. Zhang and F. Wurthner, *Angew Chem Int Ed Engl*, 2012, **51**, 6328-6348.
53. V. Percec, S. D. Hudson, M. Peterca, P. Leowanawat, E. Aqad, R. Graf, H. W. Spiess, X. Zeng, G. Ungar and P. A. Heiney, *J Am Chem Soc*, 2011, **133**, 18479-18494.
54. V. Percec, M. Peterca, T. Tadjiev, X. Zeng, G. Ungar, P. Leowanawat, E. Aqad, M. R. Imam, B. M. Rosen, U. Akbey, R. Graf, S. Sekharan, D. Sebastiani, H. W. Spiess, P. A. Heiney and S. D. Hudson, *J. Am. Chem. Soc.*, 2011, **133**, 12197-12219.
55. X. Zhang, D. Gorl, V. Stepanenko and F. Wurthner, *Angew. Chem. Int. Ed.*, 2014, **53**, 1270-1274.
56. D. Gorl, B. Soberats, S. Herbst, V. Stepanenko and F. Wurthner, *Chem. Sci.*, 2016, **7**, 6786-6790.
57. V. Grande, B. Soberats, S. Herbst, V. Stepanenko and F. Wurthner, *Chem. Sci.*, 2018, **9**, 6904-6911.
58. Y. Xiao, X. Tan, W. Xing, K. Zhao, B. Zhang and X. Cheng, *J. Mater. Chem. C*, 2018, **6**, 10782-10792.
59. H. Wang, Y. Han, W. Yuan, M. Wu and Y. Chen, *Chem Asian J*, 2018, **13**, 1173-1179.
60. H. Chen, R. Zhang, H. Gao, H. Cheng, H. Fang and X. Cheng, *Dyes and Pigments*, 2018, **149**, 512-520.
61. K. K. Kartha, N. K. Allampally, A. T. Politi, D. D. Prabhu, H. Ouchi, R. Q. Albuquerque, S. Yagai and G. Fernandez, *Chem. Sci.*, 2019, **10**, 752-760.
62. T. Nakanishi, *Chem. Commun.*, 2010, **46**, 3425-3436.
63. M. J. Hollamby, M. Karny, P. H. H. Bomans, N. A. J. M. Sommerdjik, A. Saeki, S. Seki, H. Minamikawa, I. Grillo, B. R. Pauw, P. Brown, J. Eastoe, H. Möhwald and T. Nakanishi, *Nature Chemistry*, 2014, **6**, 690-696.
64. F. Lu, E. A. Neal and T. Nakanishi, *Acc. Chem. Res.*, 2019, **52**, 1834-1843.
65. M. Yoshio, R. Konishi, T. Sakamoto and T. Kato, *New J. Chem.*, 2013, **37**, 143-147.
66. H. Cheng, R. Zhang, T. Li, X. Peng, M. Xia, Y. Xiao and X. Cheng, *New J. Chem.*, 2017, **41**, 8443-8450.
67. H. Cheng, H. Gao, Y. Xiao, B. Zhang, W. Xing and X. Cheng, *J. Mol. Liq.*, 2018, **264**, 691-698.
68. W. Xing, Y. Xiao, K. Zhao, T. Kong and X. Cheng, *J. Mol. Liq.*, 2018, **272**, 1-7.
69. H.-F. Cheng, W. Xing, B. Zhang, J. Yu and X.-H. Cheng, *Tetrahedron*, 2018, **74**, 2735-2742.
70. C. Zhang, T. Zhang, N. Ji, Y. Zhang, B. Bai, H. Wang and M. Li, *Soft Matter*, 2016, **12**, 1525-1533.
71. C. Zhang, X. Che, T. Zhang, B. Bai, H. Wang and M. Li, *New J. Chem.*, 2017, **41**, 9482-9488.
72. H.-J. Kim, S.-K. Kang, Y.-K. Lee, C. Seok, J.-K. Lee, W.-C. Zin and M. Lee, *Angew. Chem. Int. Ed.*, 2010, **49**, 8471-8475.
73. H.-J. Kim, F. Liu, J.-H. Ryu, S.-K. Kang, X. Zeng, G. Ungar, J.-K. Lee, W.-C. Zin and M. Lee, *J. Am. Chem. Soc.*, 2012, **134**, 13871-13880.
74. X. Liu, H. Li, Y. Kim and M. Lee, *Chem. Commun.*, 2018, **54**, 3102-3105.
75. Y. Liu, K. Zhong, Z. Li, Y. Wang, T. Chen, M. Lee and L. Y. Jin, *Polym. Chem.*, 2015, **6**, 7395-7401.
76. S. You, K. Zhong and L. Y. Jin, *Soft Matter*, 2017, **13**, 3334-3340.
77. Y. Yang, K. Zhong, T. Chen and L. Y. Jin, *Langmuir*, 2018, **34**, 10613-10621.
78. A. P. Sivadas, D. S. S. Rao, N. S. S. Kumar, D. D. Prabhu, S. Varghese, C. N. Ramachandran, R. M. Ongungal, S. Krishna Prasad and S. Das, *J. Phys. Chem. B*, 2017, **121**, 1922-1929.
79. B. Pradhan, M. Gupta, S. K. Pal and A. S. Achalkumar, *J. Mater. Chem. C*, 2016, **4**, 9669-9673.
80. B. Pradhan, R. K. Gupta, S. K. Pathak, J. De, S. K. Pal and A. S. Achalkumar, *New J. Chem.*, 2018, **42**, 3781-3798.
81. R. A. Reddy and C. Tschierske, *J. Mater. Chem.*, 2006, **16**, 907-961.
82. J. Etxebarria and M. Blanca Ros, *J. Mater. Chem.*, 2008, **18**, 2919-2926.
83. S.-C. Lin, T.-F. Lin, R.-M. Ho, C.-Y. Chang and C.-S. Hsu, *Adv. Funct. Mater.*, 2008, **18**, 3386-3394.
84. S. C. Lin, R. M. Ho, C. Y. Chang and C. S. Hsu, *Chem. Eur. J.*, 2012, **18**, 9091-9098.
85. M. Cano, A. Sanchez-Ferrer, J. L. Serrano, N. Gimeno and M. B. Ros, *Angew. Chem. Int. Ed.*, 2014, **53**, 13449-13453.
86. L. E. Hough, H. T. Jung, D. Krüerke, M. S. Heberling, M. Nakata, C. D. Jones, D. Chen, D. R. Link, J. Zasadzinski, G. Heppke, J. P. Rabe, W. Stocker, E. Körblova, D. M. Walba, M. A. Glaser and N. A. Clark, *Science*, 2009, **325**, 456-460.
87. K. V. Le, H. Takezoe and F. Araoka, *Adv. Mater.*, 2017, **29**, 1602737.
88. T. Otani, F. Araoka, K. Ishikawa and H. Takezoe, *J. Am. Chem. Soc.*, 2009, **131**, 12368-12372.
89. D. Chen, C. Zhu, H. Wang, J. E. Maclennan, M. A. Glaser, E. Korblova, D. M. Walba, J. A. Rego, E. A. Soto-Bustamante and N. A. Clark, *Soft Matter*, 2013, **9**, 462-471.
90. J. Matraszek, N. Topnani, N. Vaupotic, H. Takezoe, J. Mieczkowski, D. Pociecha and E. Gorecka, *Angew. Chem. Int. Ed.*, 2016, **55**, 3468-3472.
91. R. J. Mandle, *Soft Matter*, 2016, **12**, 7883-7901.
92. A. Zep, M. Salamonczyk, N. Vaupotic, D. Pociecha and E. Gorecka, *Chem. Commun.*, 2013, **49**, 3119-3121.
93. A. Zep, K. Sitkowska, D. Pociecha and E. Gorecka, *J. Mater. Chem. C*, 2014, **2**, 2323-2327.

94. M. M., A. Roy and V. Prasad, *New J. Chem.*, 2017, **41**, 11576-11583.
95. H. M. Diab, A. M. Abdelmoniem, M. R. Shaaban, I. A. Abdelhamid and A. H. M. Elwahy, *RSC Adv.*, 2019, **9**, 16606-16682.
96. P. J. Stals, J. C. Everts, R. de Bruijn, I. A. Filot, M. M. Smulders, R. Martin-Rapun, E. A. Pidko, T. F. de Greef, A. R. Palmans and E. W. Meijer, *Chem. Eur. J.*, 2010, **16**, 810-821.
97. T. Mes, S. Cantekin, D. W. R. Balkenende, M. M. M. Frissen, M. A. J. Gillissen, B. F. M. De Waal, I. K. Voets, E. W. Meijer and A. R. A. Palmans, *Chem.-Eur. J.*, 2013, **19**, 8642-8649.
98. P. J. M. Stals, J. F. Haveman, R. Martín-Rapún, C. F. C. Fitié, A. R. A. Palmans and E. W. Meijer, *J. Mater. Chem.*, 2009, **19**, 124-130.
99. M. Garcia-Iglesias, B. F. de Waal, I. de Feijter, A. R. Palmans and E. W. Meijer, *Chem. Eur. J.*, 2015, **21**, 377-385.
100. J. A. Berrocal, F. Di Meo, M. Garcia-Iglesias, R. P. Gosens, E. W. Meijer, M. Linares and A. R. Palmans, *Chem. Commun.*, 2016, **52**, 10870-10873.
101. A. Desmarchelier, B. G. Alvarenga, X. Caumes, L. Dubreucq, C. Troufflard, M. Tessier, N. Vanthuyne, J. Ide, T. Maistriaux, D. Beljonne, P. Brocorens, R. Lazzaroni, M. Raynal and L. Bouteiller, *Soft Matter*, 2016, **12**, 7824-7838.
102. Y. J. Choi, D. Y. Kim, M. Park, W. J. Yoon, Y. Lee, J. K. Hwang, Y. W. Chiang, S. W. Kuo, C. H. Hsu and K. U. Jeong, *ACS Appl. Mater. Int.*, 2016, **8**, 9490-9498.
103. K. Sato, Y. Itoh and T. Aida, *J. Am. Chem. Soc.*, 2011, **133**, 13767-13769.
104. K. Sato, Y. Itoh and T. Aida, *Chem. Sci.*, 2014, 5, 136-140.
105. S. Varghese, N. S. S. Kumar, A. Krishna, D. S. S. Rao, S. K. Prasad and S. Das, *Adv. Funct. Mater.*, 2009, **19**, 2064-2073.
106. D. D. Prabhu, N. S. Kumar, A. P. Sivadas, S. Varghese and S. Das, *J. Phys. Chem. B*, 2012, **116**, 13071-13080.
107. S. K. Pathak, B. Pradhan, R. K. Gupta, M. Gupta, S. K. Pal and A. S. Achalkumar, *J. Mater. Chem. C*, 2016, **4**, 6546-6561.
108. S. Nath, S. K. Pathak, J. De, S. K. Pal and A. S. Achalkumar, *Mol. Syst. Des. Eng.*, 2017, **2**, 478-489.
109. P. Agarwala and D. Kabra, *J. Mater. Chem. A*, 2017, **5**, 1348-1373.
110. Y. Domoto, E. Busseron, M. Maaloum, E. Moulin and N. Giuseppone, *Chem. Eur. J.*, 2015, **21**, 1938-1948.
111. I. Nyrkova, E. Moulin, J. J. Armao, M. Maaloum, B. Heinrich, M. Rawiso, F. Niess, J.-J. Cid, N. Jouault, E. Buhler, A. N. Semenov and N. Giuseppone, *ACS Nano*, 2014, **8**, 10111-10124.
112. K. Kubo, Y. Moriyama, S. Ujiie and A. Mori, *Chem. Lett.*, 2015, **44**, 984-986.
113. T. Wohrle, I. Wurzbach, J. Kirres, A. Kostidou, N. Kapernaum, J. Litterscheidt, J. C. Haenle, P. Staffeld, A. Baro, F. Giesselmann and S. Laschat, *Chem. Rev.*, 2016, **116**, 1139-1241.
114. S. K. Pal, S. Setia, B. S. Avinash and S. Kumar, *Liq. Cryst.*, 2013, **40**, 1769-1816.
115. A. Kotlewski, B. Norder, W. F. Jager, S. J. Picken and E. Mendes, *Soft Matter*, 2009, **5**, 4905-4913.
116. A. A. Khan, M. A. Kamarudin, M. M. Qasim and T. D. Wilkinson, *Electrochimica Acta*, 2017, **244**, 162-171.
117. B. S. Avinash, V. Lakshminarayanan, S. Kumar and J. K. Vij, *Chem. Commun.*, 2013, **49**, 978-980.
118. A. B. Shivanandareddy, M. Kumar, A. Gowda and S. Kumar, *J. Mol. Liq.*, 2017, **244**, 1-6.
119. V. Bhalla, H. Singh, M. Kumar and S. K. Prasad, *Langmuir*, 2011, **27**, 15275-15281.
120. M. Kaller, C. Deck, A. Meister, G. Hause, A. Baro and S. Laschat, *Chem. Eur. J.*, 2010, **16**, 6326-6337.
121. B. Zhao, B. Liu, R. Q. Png, K. Zhang, K. A. Lim, J. Luo, J. Shao, P. K. H. Ho, C. Chi and J. Wu, *Chem. Mater.*, 2010, **22**, 435-449.
122. J. Szydłowska, P. Krzyczkowska, M. Salamończyk, E. Górecka, D. Pociecha, B. Maranowski and A. Krówczyński, *J. Mater. Chem. C*, 2013, **1**, 6883-6889.
123. M.-C. Tzeng, S.-C. Liao, T.-H. Chang, S.-C. Yang, M.-W. Weng, H.-C. Yang, M. Y. Chiang, Z. Kai, J. Wu and C. W. Ong, *J. Mater. Chem.*, 2011, **21**, 1704-1712.
124. S. Diring, F. Camerel, B. Donnio, T. Dintzer, S. Toffanin, R. Capelli, M. Muccini and R. Ziessel, *J. Am. Chem. Soc.*, 2009, **131**, 18177-18185.
125. A.-M. Caminade, D. Yan and D. K. Smith, *Chem. Soc. Rev.*, 2015, **44**, 3870-3873.
126. G.-C. Kuang, Y. Ji, X.-R. Jia, Y. Li, E.-Q. Chen and Y. Wei, *Chem. Mater.*, 2008, **20**, 4173-4175.
127. G.-C. Kuang, X.-R. Jia, M.-J. Teng, E.-Q. Chen, W.-S. Li and Y. Ji, *Chem. Mater.*, 2011, **24**, 71-80.
128. G. Kuang, Y. Ji, X. Jia, E. Chen, M. Gao, J. Yeh and Y. Wei, *Chem. Mater.*, 2009, **21**, 456-462.
129. M. Seo, J. H. Kim, J. Kim, N. Park, J. Park and S. Y. Kim, *Chem. Eur. J.*, 2010, **16**, 2427-2441.
130. E. Fedeli, A. Lancelot, J. L. Serrano, P. Calvo and T. Sierra, *New J. Chem.*, 2015, **39**, 1960-1967.
131. I. Gracia, J. L. Serrano, J. Barberá and A. Omenat, *RSC Adv.*, 2016, **6**, 39734-39740.
132. S. Hernández-Ainsa, J. Barberá, M. Marcos and J. L. Serrano, *Soft Matter*, 2011, **7**, 2560-2568.
133. S. Hernandez-Ainsa, E. Fedeli, J. Barbera, M. Marcos, T. Sierra and J. L. Serrano, *Soft Matter*, 2014, **10**, 281-289.
134. H. H. Nguyen, C. V. Serrano, P. Lavedan, D. Goudouneche, A. F. Mingotaud, N. Lauth-de Viguerie and J. D. Marty, *Nanoscale*, 2014, **6**, 3599-3610.
135. E. Fedeli, S. Hernández-Ainsa, A. Lancelot, R. González-Pastor, P. Calvo, T. Sierra and J. L. Serrano, *Soft Matter*, 2015, **11**, 6009-6017.
136. Y. Liao and C.-M. Dong, *J. Pol. Sci. A Pol. Chem.*, 2012, **50**, 1834-1843.
137. H. Wu, L. Zhang, Y. Xu, Z. Ma, Z. Shen, X. Fan and Q. Zhou, *J. Pol. Sci. A Pol. Chem.*, 2012, **50**, 1792-1800.
138. L. Chen, Y. Yuan, G. Zhong, J. Li and H. Zhang, *Polymer*, 2017, **132**, 51-58.
139. Y. Gao, X. Li, L. Hong and G. Liu, *Macromolecules*, 2012, **45**, 1321-1330.
140. X. Li, Y. Gao, X. Xing and G. Liu, *Macromolecules*, 2013, **46**, 7436-7442.
141. X. Li, B. Jin, Y. Gao, D. W. Hayward, M. A. Winnik, Y. Luo and I. Manners, *Angew. Chem. Int. Ed.,* 2016, **55**, 11392-11396.
142. S. p. Boissé, J. Rieger, A. l. Di-Cicco, P.-A. Albouy, C. Bui, M.-H. Li and B. Charleux, *Macromolecules*, 2009, **42**, 8688-8696.
143. B. Yan, X. Tong, P. Ayotte and Y. Zhao, *Soft Matter*, 2011, **7**, 10001-10009.
144. S. Honda, M. Koga, M. Tokita, T. Yamamoto and Y. Tezuka, *Pol. Chem.*, 2015, **6**, 4167-4176.
145. Z. H. Guo, X. F. Liu, J. S. Hu, L. Q. Yang and Z. P. Chen, *Nanomaterials*, 2017, **7**, 169.
146. P. Liu, J. Liang, S. Chen and H. Zhang, *RSC Adv.*, 2014, **4**, 49028-49039.
147. J. Zhang, X. F. Chen, H. B. Wei and X. H. Wan, *Chem. Soc. Rev.*, 2013, **42**, 9127-9154.
148. L. Jia and M.-H. Li, *Liq. Cryst.*, 2014, **41**, 368-384.
149. D. Wu, Y. Huang, F. Xu, Y. Mai and D. Yan, *J. Pol. Sci. A Pol. Chem.*, 2017, **55**, 1459-1477.

150. Y. Deng, J. Ling and M. H. Li, *Nanoscale*, 2018, **10**, 6781-6800.
151. C. K. Wong, A. F. Mason, M. H. Stenzel and P. Thordarson, *Nat. Comm.*, 2017, **8**, 1240.
152. Y. Zhou, V. Briand, N. Sharma, S.-k. Ahn and R. Kasi, *Materials*, 2009, **2**, 636-660.
153. L. Hosta-Rigau, Y. Zhang, B. M. Teo, A. Postma and B. Stadler, *Nanoscale*, 2013, **5**, 89-109.
154. F. Ercole, M. R. Whittaker, J. F. Quinn and T. P. Davis, *Biomacromolecules*, 2015, **16**, 1886-1914.
155. H. Yang, L. Jia, C. Zhu, A. Di-Cicco, D. Levy, P.-A. Albouy, M.-H. Li and P. Keller, *Macromolecules*, 2010, **43**, 10442-10451.
156. L. Jia, D. Lévy, D. Durand, M. Impéror-Clerc, A. Cao and M.-H. Li, *Soft Matter*, 2011, **7**, 7395-7403.
157. L. Jia, M. Liu, A. Di Cicco, P. A. Albouy, B. Brissault, J. Penelle, S. Boileau, V. Barbier and M. H. Li, *Langmuir*, 2012, **28**, 11215-11224.
158. X. Zhang, S. Boissé, C. Bui, P.-A. Albouy, A. Brûlet, M.-H. Li, J. Rieger and B. Charleux, *Soft Matter*, 2012, **8**, 1130-1141.
159. L. Jia, D. Cui, J. Bignon, A. Di Cicco, J. Wdzieczak-Bakala, J. Liu and M. H. Li, *Biomacromolecules*, 2014, **15**, 2206-2217.
160. L. Zhou, D. Zhang, S. Hocine, A. Pilone, S. Trépout, S. Marco, C. Thomas, J. Guo and M.-H. Li, *Pol. Chem.*, 2017, **8**, 4776-4780.
161. L. Li, F. Zhou, Y. Li, X. Chen, Z. Zhang, N. Zhou and X. Zhu, *Langmuir*, 2018, **34**, 11034-11041.
162. B. Xu, R. Piñol, M. Nono-Djamen, S. Pensec, P. Keller, P.-A. Albouy, D. Lévy and M.-H. Li, *Faraday Discuss.*, 2009, **143**, 235-250.
163. K. Ferji, C. Nouvel, J. Babin, M.-H. Li, C. Gaillard, E. Nicol, C. Chassenieux and J.-L. Six, *ACS Macro Letters*, 2015, **4**, 1119-1122.
164. Y. Xie, X. Liu, Z. Hu, Z. Hou, Z. Guo, Z. Chen, J. Hu and L. Yang, *Nanomaterials*, 2018, **8**, 195.
165. J. Tang, R. M. Berry and K. C. Tam, *Biomacromolecules*, 2016, **17**, 1748-1756.
166. J. Yang, R. Piñol, F. Gubellini, D. Lévy, P.-A. Albouy, P. Keller and M.-H. Li, *Langmuir*, 2006, **22**, 7907-7911.
167. S. Hocine, A. Brûlet, L. Jia, J. Yang, A. Di Cicco, L. Bouteiller and M.-H. Li, *Soft Matter*, 2011, **7**, 2613-2623.
168. S. Hocine, D. Cui, M. N. Rager, A. Di Cicco, J. M. Liu, J. Wdzieczak-Bakala, A. Brulet and M. H. Li, *Langmuir*, 2013, **29**, 1356-1369.
169. N. Topnani, M. Kašpar, V. Hamplová, E. Gorecka and D. Pociecha, *J. Mater. Chem. C*, 2014, **2**, 10357-10361.
170. S. Lin, Y. Wang, C. Cai, Y. Xing, J. Lin, T. Chen and X. He, *Nanotechnology*, 2013, **24**, 085602.
171. R.-B. Wei, X.-G. Wang and Y.-N. He, *Chin. Chem. Lett.*, 2015, **26**, 857-861.
172. J. del Barrio, L. Oriol, C. Sánchez, J. L. Serrano, A. Di Cicco, P. Keller and M.-H. Li, *J. Am. Chem. Soc.*, 2010, **132**, 3762-3769.
173. E. Blasco, J. del Barrio, C. Sánchez-Somolinos, M. Piñol and L. Oriol, *Pol. Chem.*, 2013, **4**, 2246-2254.
174. P. Wang, S. Cao, Y. Zhao, T. Iyoda and A. Chen, *Macromol. Chem. Phys.*, 2017, **218**, 1700148.
175. T. Kato, J. Uchida, T. Ichikawa and T. Sakamoto, *Angew. Chem. Int. Ed.*, 2018, **57**, 4355-4371.